Synchronization Techniques for All Digital 16-ary QAM Receivers Operating over Land Mobile Satellite Links

P. Fines, A.H. Aghvami
Communications Research Group
Department of Electrical and Electronic Engineering
King's College, University of London
Strand, London WC2R LS, U.K.
Phone: 44 71 873 2898
FAX: 44 71 836 4781

ABSTRACT

In this paper, the performance of a low bit rate (64Kb/s) all digital 16-ary Differentially Encoded Quadrature Amplitude Modulation (16-DEQAM) demodulator operating over a mobile satellite channel, is considered. The synchronization and detection techniques employed to overcome the Rician channel impairments, are described. The acquisition and steady state performances of this modem, are evaluated by computer simulation over AWGN and Rician channels. The results verify the suitability of the 16-DEQAM transmission over slowly faded and/or mildly faded channels.

INTRODUCTION

Because of the limited bandwidth availability for digital satellite communications, the current trend has been towards improving the spectrum efficiency of satellite systems by employing high spectrally efficient modulation schemes. Recently 16-ary QAM has received much attention as a candidate for future satellite communications. However, because of the non-constant nature of their amplitudes, 16-ary QAM signals are very sensitive to the non-linearities of satellite channels. That is why 16-ary QAM has not been used in the existing satellite communications systems. With the recent developments in solid-state power amplifier designs and using predistortion techniques, potential application of 16-ary QAM for future satellite systems are now becoming more recognizable.

To satisfy the power limitations and achieve optimum performance, coherent detection at the receiver, must be used. Coherent demodulation is a difficult task in a land mobile satellite environment. This is because multipath fading and Doppler frequency shifts prevent reliable derivation of a carrier reference signal. The carrier amplitude and phase vary considerably and rapidly, depending on the vehicle speed and the severity of the fading. In m-ary QAM transmissions, successful carrier amplitude tracking is equally important as carrier phase tracking. The 16-DEQAM system presented in this study employs coherent detection by means of decision directed carrier amplitude gain control and phase synchronization. Furthermore,large carrier frequency offsets and symbol timing errors have been tackled effectively.

16-DEQAM MODULATOR

The system model under investigation is shown in Fig.1. This model is the baseband equivalent to a typical land mobile satellite link which includes the modulator, the physical channel and the demodulator.

Because of the 16-QAM signal symmetry, there is a fourfold ambiguity in the data recovery. Differential encoding (DE) is used to resolve this phase ambiguity. In order to minimise the BER the assignment of bits to the symbols are such that its nearest neighbours differ in as few bits as possible (exact Gray coding is unachievable). The two most significant

bits (MSB) are differential encoded to represent the change in quadrant. The remain two bits represent the symbol points in each quadrant.

The generated 16-ary DE impulses are converted to bandlimited waveforms by filtering. The transfer function of the filters is square-root raised cosine with excess bandwidth of 50%.

CHANNEL MODEL

In this study no assumptions on carrier amplitude, frequency and phase or symbol timing synchronization are made. The channel model of Fig.1 demonstrates how synchronization errors are introduced as well as the fading and AWGN. The symbol timing errors are introduced by passing the transmitted signal through a variable delay line. Frequency offset errors represent the total local oscillators instability and inaccuracy between transmitter and receiver, as well as large Doppler shifts due to the receiver motion relative to the satellite.

The land mobile satellite channel is assumed non frequency selective for the data rates of interest, and its statistical characteristics are Rician. This fading model [1] considers two signal paths from the satellite to the mobile receiver: a line of sight (LOS) path and a scatter (multipath) path. As a result, the received signal can be modeled as the sum of two components, a direct and a diffuse one. Propagation experiments suggest that for land mobile satellite communications, if the direct path is clear the diffuse component has an rms value 10-20 dB below the direct one. In this study shadowing is not considered, and therefore, the LOS component power is constant.

The diffuse component is modeled with Rayleigh distributed envelope and uniform distributed phase. The time behavior of the fading is mainly characterized by the half of the Doppler spread:

$$f_D = f_c \frac{V}{C} \qquad (1)$$

where fc is the carrier frequency, V is the vehicle speed and C is the speed of light.

The power spectral density of the fading process is assumed according to:

$$S(f) = \begin{cases} \{1-(f/f_D)^2\}^{-1/2} , & |f| \le f_D \\ 0 , & |f| > f_D \end{cases} \qquad (2)$$

Two independent white Gaussian sources with zero mean and one sided power spectral density S_o, are filtered by the shaping filters $S(f)$ to give a complex zero mean Gaussian random process with power spectrum $S(f)$ and total power: $2S_oB_x\sigma^2$, where B_x is equivalent noise bandwidth of $S(f)$. For simplicity, the values of S_o and B_x are such that: $S_oB_x=1$.

The random process $y(t)$ results from adding the constant μ. The amplitude of the complex fading distortion process $h(t)=x(t)+jy(t)$ is the Rician distributed carrier attenuation:

$$a(t) = \{x(t)^2+y(t)^2\}^{1/2} \qquad (3)$$

The phase of the fading process $h(t)$ is:

$$b(t) = tan^{-1}\{y(t)/x(t)\} \qquad (4)$$

The severity of the fading is determined by the direct to multipath signal power ratio (Rice factor):

$$c = \mu^2/2\sigma^2 \qquad (5)$$

By selecting $c = 0$ a severely fading Rayleigh channel results. In the limit $c \rightarrow \infty$ the Rician channel reduces to the nonfading AWGN channel.

The coefficients σ and μ are scaled such that:

$$E\{a(t)^2\} = 2\sigma^2 + \mu^2 = 1 \qquad (6)$$

in order to the average transmitted bit energy (E_b) remain unaffected by the channel fading.

16-DEQAM DEMODULATOR

The demodulator incorporates all the necessary synchronization and detection processes. Synchronization is obtained at four levels: carrier amplitude frequency and phase, symbol timing.

The received signal can be expressed as:

$$r(t)=a(t)e^{j[2\pi f_e t+b(t)]}\sum_k s(k)g(t-kT-\tau)+n(t) \quad (7)$$

where, $s(k)$ is the k-th transmitted 16-ary complex symbol, $g(t)$ is symbol pulse, T is the symbol time period, τ is the symbol timing error, f_e is the carrier frequency offset, $a(t)$ and $b(t)$ are the carrier attenuation and phase error introduced by the fading as is given by (3) and (4), and $n(t)$ is complex AWGN with one sided spectral density N_o.

In (7) the effects of fading and synchronization errors are shown clearly with simple mathematical terms. The mathematical model of the demodulator required in order to retrieve the transmitted bits from $r(t)$ is illustrated in Fig.2. The input signal is a sampled version of $r(t)$. To reduce the computing burden, the sampling rate is minimized at all stages. At the demodulator input the signal $r(t)$ is represented by its samples obtained with a sampling rate of four times the symbol rate. In order to simplify the hardware, the sampling phase is not synchronized with the symbol rate (nonsynchronous sampling). The four synchronization levels employ feedback loop structure and all of them have three elements: parameter error detector, filtering of the estimated error and parameter adjuster [2].

Carrier Frequency Synchronization

A second order phase locked loop (PLL) will be unable to phase lock in the presence of large carrier frequency offset. For that an automatic frequency control (AFC) loop is used to reduce the initial frequency error and then a PLL removes the remaining error. This strategy allows fast and reliable carrier phase acquisition. In both cases the frequency errors are corrected by frequency translation of the incoming signal $r(t)$. The AFC loop is driven by a frequency error detector which is described in ref. [3]. The frequency error is computed as:

$$f_e = |r_+(t)|^2 - |r_-(t)|^2 \quad (9)$$

with,

$$r_\pm(t) = r(t) \otimes g(t)e^{\pm j2\pi F_s t} \quad (10)$$

where $\otimes$ denotes convolution, $g(t)$ is the impulse response of the data filters and F_s is the symbol rate. $r_\pm(t)$ satisfy the conditions found in [3] for pattern jitter free frequency error detector which ensures improved performance. With small frequency error, the required frequency translation is controlled by the phase error detector similar to the case of a second order PLL. In both cases the estimated frequency error is integrated in order to control the Number Controlled Oscillator (NCO). The loop bandwidths of the AFC and PLL are controlled by the coefficients **D** and **C** as shown in Fig.2.

Symbol Timing Synchronization

Since nonsynchronous sampling is employed, correct adjusted samples are computed by interpolation through the available samples. This process is equivalent to a variable delay line in the signal path. Interpolation is implemented by convolution of the incoming signal $r(t)$ with an interpolating function:

$$r(t-\tau_d) = r(t) \otimes d(t+\tau_d) \quad (11)$$

where $\otimes$ denotes convolution, $d(t)$ is the interpolating function and τ_d is the time delay. The interpolator is implemented by a FIR transversal filter and the required delay is selected by changing its coefficients.For efficient implementation, the timing correction resolution is 1.5% of the symbol period. The timing phase error is computed by [3]:

$$\tau_e = \frac{1}{2\pi} arg\left\{ \int_{LT^+}^{LT} r_+(t)r_-^*(t)e^{-j2\pi F_s t}dt \right\} \quad (12)$$

where * denotes complex conjugation, LT is a time period of L symbols and, $r_\pm(t)$ and F_s as in (10). The computed timing error τ_e is an unbiased estimate of the timing error, free of pattern noise and carrier amplitude,frequency and phase independent. The error τ_e is integrated and then is used for the appropriate selection of interpolator coefficients. The response of the loop is controlled by the coefficient **A** of Fig.2. Finally, hangup is avoided because the timing correction resolution is discrete and the error τ_e is computed by (12) every $2L$ symbols.

Carrier Amplitude Control

An automatic gain control (AGC) loop is employed to compensate the short term fading attenuation. The long term attenuation is assumed to be handled in the RF and IF sections by a more standard average energy type AGC loop. The carrier amplitude error gain is computed as:

$$A_e = |C_n|/|\hat{C}_n| \qquad (13)$$

where C_n and $\hat{C}_n$ are the n-th complex sample at the input and output of the decision unit. When the signal level and the receiver attenuation are expressed as a logarithm, the AGC loop becomes a linear system. The response of the loop is controlled by the coefficient **E** of Fig.2.

Carrier Phase Synchronization

The phase error is computed as:

$$\phi_e = arg\{C_n \hat{C}_n^*\} \qquad (14)$$

where * is complex conjugation, C_n and $\hat{C}_n$ as in (13). (14) can be implemented efficiently by a look-up table [4]. The estimated phase error is integrated and then is used to correct the phase of the matched filter sample. The response of the loop is controlled by the coefficient **B** of Fig.2. At this point, a first order loop is sufficient as long as the frequency error is corrected in a separate loop [2].

COMPUTER SIMULATION RESULTS

Acquisition Performance

The acquisition performance of the system is computed in terms of the time period required by the system to obtain synchronization starting from practical maximum timing, frequency and gain errors. Good acquisition performance will also guarantee better steady performance in terms of BER because the reacquisition of the system after a deep fade will be faster causing less errors. The convergence of the system operating over a AWGN channel with E_b/N_o=10dB, starting with a timing error of 50% of the symbol time period, 1.6KHz carrier frequency offset and 6dB signal gain, is shown in Fig.3. The timing recovery loop locks in less than 300 symbol periods. The AFC loop reduces the frequency offset in less than 300 symbols. The PLL and AGC lock in less than 40 symbols giving a total phase lock period of 340 symbols.

Steady State Performance

For a AWGN channel, the BER performance shown in Fig.4 a), demonstrates the small degradation caused by the system.

The BER performance over a Rician channel is shown in Fig.4 b) and c) for various channel parameters. From these figures it is evident that this system is suitable for channels that are not severely faded or vary slowly because of their relaxed requirements in amplitude control and phase synchronization.

CONCLUSIONS

The structure of a low bit rate 16-DEQAM coherent demodulator suitable for all digital implementation is given. Its evaluated acquisition and BER performances over AWGN and Rician channel show the suitability of this bandwidth efficient modulation scheme over mildly faded channels. The main source of degradation was found to be the necessity of good amplitude as well as phase tracking mainly during fast and deep fades.

REFERENCES

1. Davarian, F. 1987. Channel Simulation to Facilitate Mobile Satellite Communications Research. IEEE Trans. Commun. VOL. COM-35, NO. 1, pp. 47-56.

2. Gardner,F.M. 1988.Demodulator reference recovery techniques suited for digital implementation. Final report ESTEC Contract 6847/86/NL/DG.

3. Alberty, T., Hespelt, V., 1989. A new pattern jitter free frequency error detector. IEEE Trans. Commun., VOL. COM-37, NO. 2, pp. 159-163.

4. Fines, P., Aghvami, A. H., 1990. Implementation of a 16-ary QAM Demodulator for Medium Data Rates. Accepted for publication at the IEE Fifth International Conference on 'Radio Receivers and Associated Systems', Cambridge, July 1990.

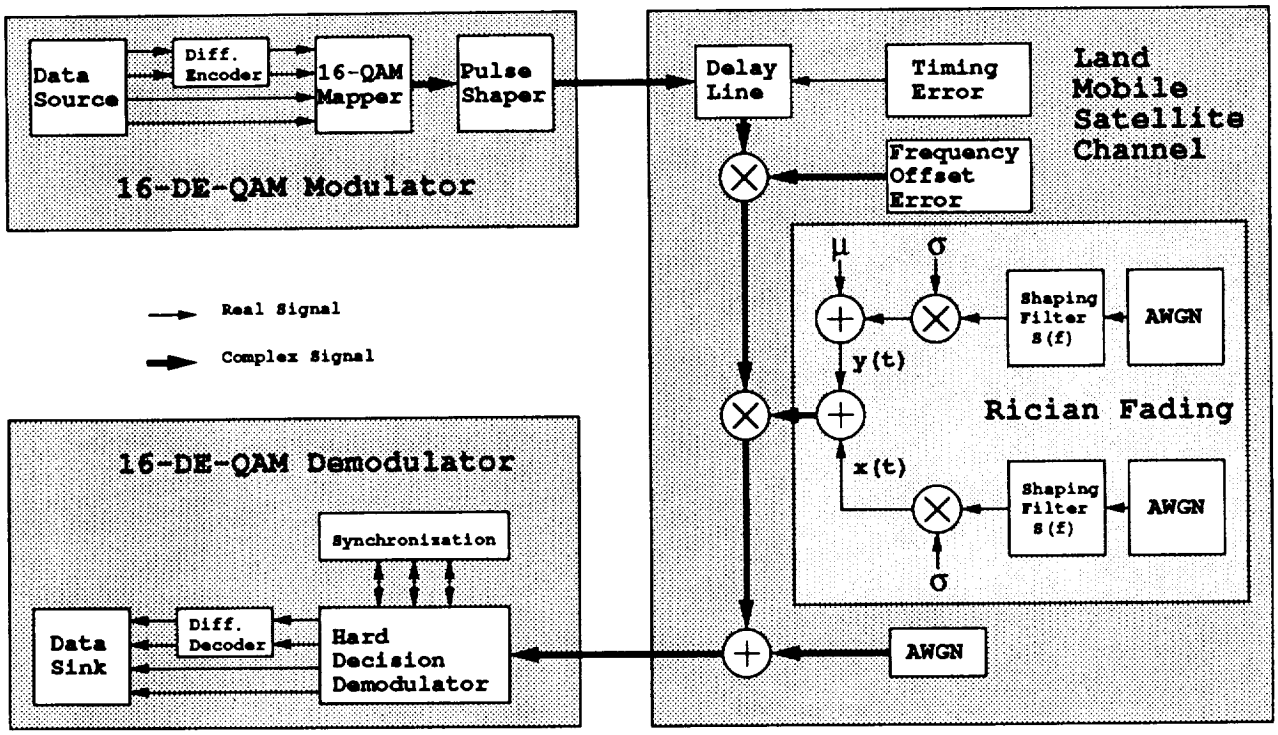

Fig.1 System model under consideration

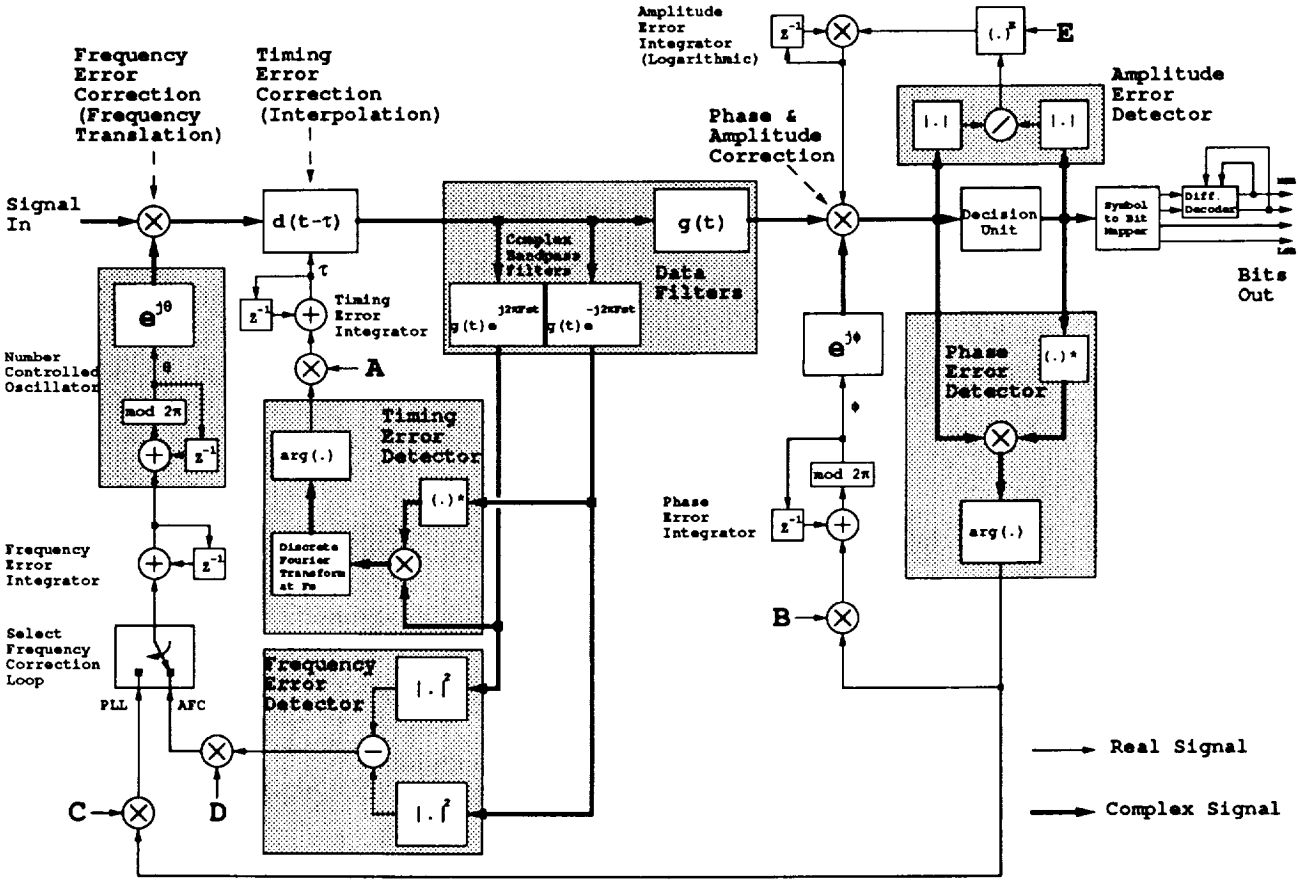

Fig.2 16-DE-QAM All Digital Demodulator

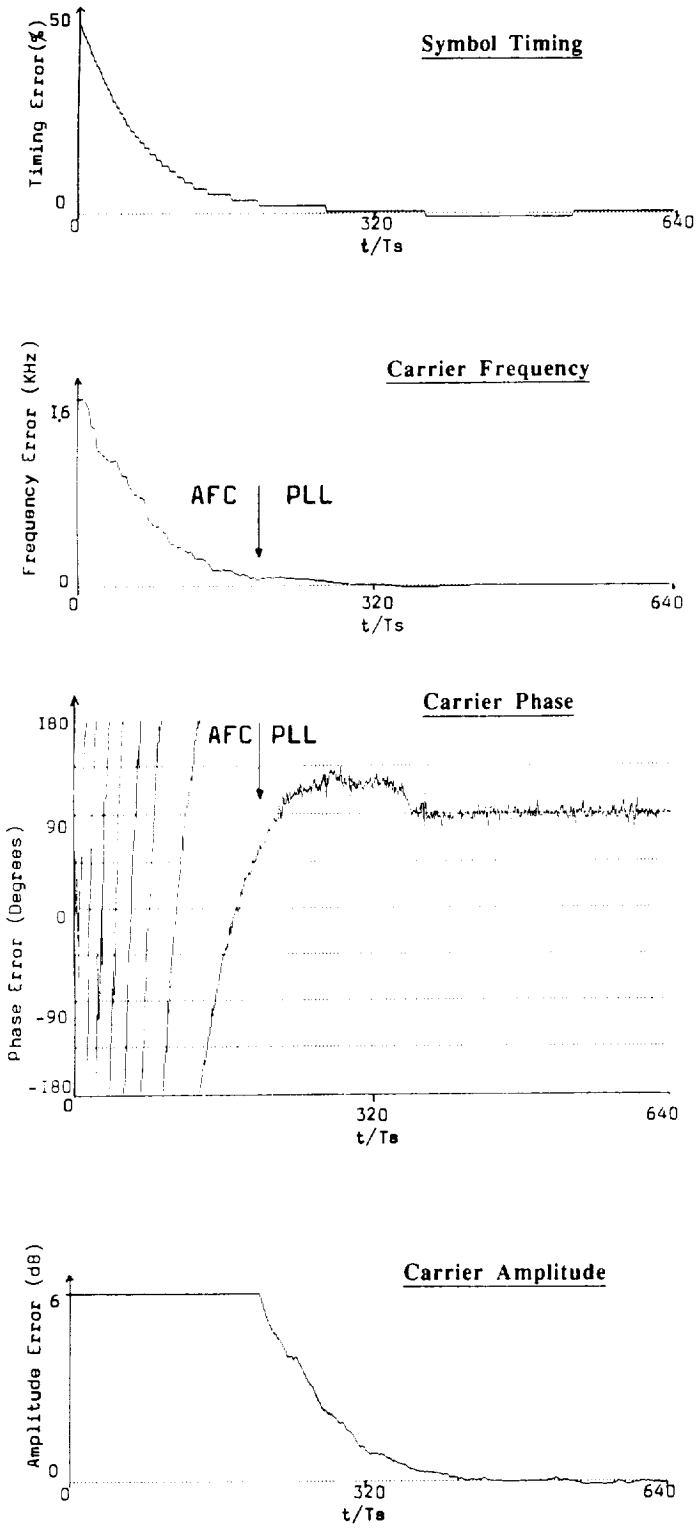

Fig.3 Acquisition performance (E_b/N_o = 10 dB)

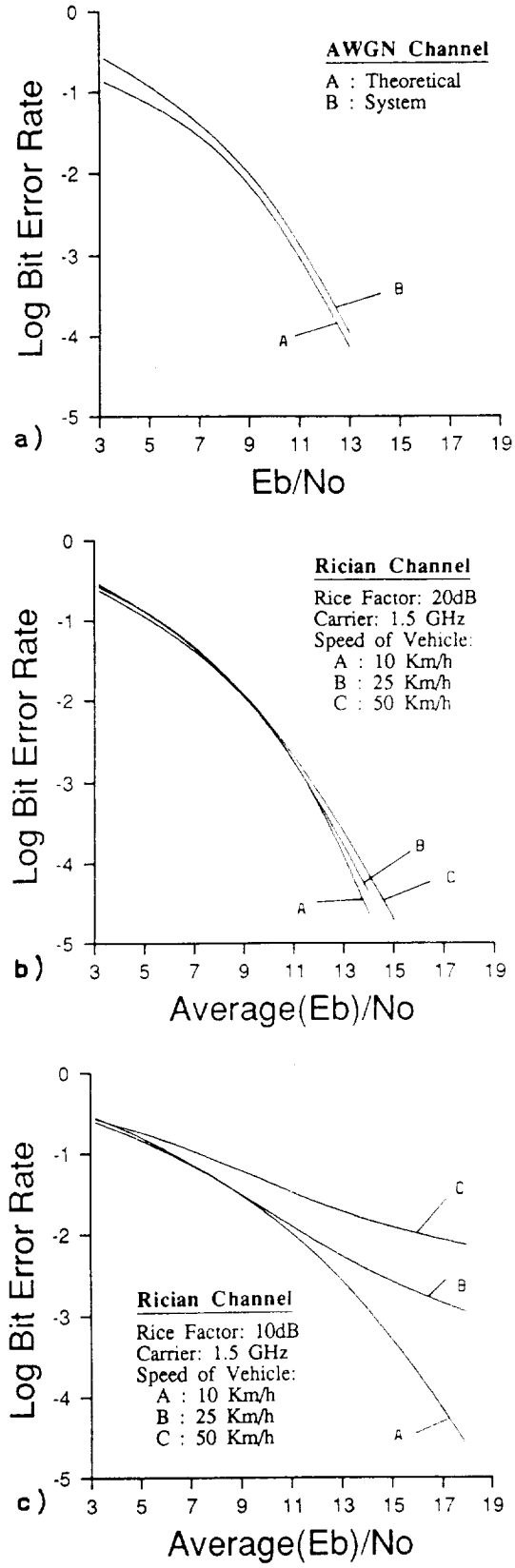

Fig.4. BER over AWGN and Rician Channels